Cellular/Molecular

Localized Loss of Ca^{2+} Homeostasis in Neuronal Dendrites Is a Downstream Consequence of Metabolic Compromise during Extended NMDA Exposures

Thomas A. Vander Jagt, John A. Connor, and C. William Shuttleworth
Department of Neurosciences, University of New Mexico School of Medicine, Albuquerque, New Mexico 87131

Excessive Ca^{2+} loading is central to most hypotheses of excitotoxic neuronal damage. We examined dendritic Ca^{2+} signals in single CA1 neurons, injected with fluorescent indicators, after extended exposures to a low concentration of NMDA (5 μM). As shown previously, NMDA produces an initial transient Ca^{2+} elevation of several micromolar, followed by recovery to submicromolar levels. Then after a delay of ~20–40 min, a large Ca^{2+} elevation appears in apical dendrites and propagates to the soma. We show here that this large delayed Ca^{2+} increase is required for ultimate loss of membrane integrity. However, transient removal of extracellular Ca^{2+} for varying epochs before and after NMDA exposure does not delay the propagation of these events. In contrast to compound Ca^{2+} elevations, intracellular Na^+ elevations are monophasic and were promptly reversed by the NMDA receptor antagonist MK-801 [(+)-5-methyl-10,11-dihydro-5*H*-dibenzo [a,d] cyclohepten-5,10-imine maleate]. MK-801 applied after the transient Ca^{2+} elevations blocked the delayed propagating Ca^{2+} increase. Even if applied after the propagating response was visualized, MK-801 restored resting Ca^{2+} levels. Propagating Ca^{2+} increases in dendrites were delayed or prevented by (1) reducing extracellular Na^+, (2) injecting ATP together with the Ca^{2+} indicator, or (3) provision of exogenous pyruvate. These results show that extended NMDA exposure initiates degenerative signaling generally in apical dendrites. Although very high Ca^{2+} levels can report the progression of these responses, Ca^{2+} itself may not be required for the propagation of degenerative signaling along dendrites. In contrast, metabolic consequences of sustained Na^+ elevations may lead to failure of ionic homeostasis in dendrites and precede Ca^{2+}-dependent cellular compromise.

Key words: **excitotoxicity; CA1; hippocampus; sodium ion; ATP; MK-801; brain slice**

Introduction

Overstimulation of glutamate receptors occurs during pathological conditions as a consequence of inappropriate transmitter release and/or compromised glutamate uptake (Olney, 1978; Choi, 1988a). As a consequence, multiple types of glutamate receptor are strongly activated, but, among these, the NMDA subtype has received particular attention in excitotoxicity (Simon et al., 1984; Choi, 1988b; Wahlestedt et al., 1993). Partial depolarization and relief of Mg^{2+} block after ischemic injuries may result in persistent low-level NMDA receptor activation (Novelli et al., 1988; Hori and Carpenter, 1994) and could contribute to increases in infarct size that occur after stroke injury *in vivo*. From studies of cultured neurons, excessive Ca^{2+} loading has been demonstrated after sustained NMDA exposures, and this Ca^{2+} overload has become central to most hypotheses of excitotoxic neuronal injury (Choi, 1988b; Arundine and Tymianski, 2003). NMDA receptor activation also results in substantial intracellular Na^+ loading, and it has long been suggested that consequences of Na^+ accumulation could be a significant contributor to neuronal injury (Rothman, 1985; Olney et al., 1986). Na^+ extrusion by Na^+/K^+/ATPase is a major consumer of neuronal energy (Attwell and Laughlin, 2001), and ATP depletion that results from excessive Na^+ entry could contribute to neuronal injury (Novelli et al., 1988; Fried et al., 1995).

ATP depletion may underlie Ca^{2+} overload after exposure of neuronal cultures to glutamate receptor agonists in neuronal cultures. As reviewed by Nicholls et al. (2007), intracellular Ca^{2+} accumulation and mitochondrial reactive oxygen species production has been suggested to cause unregulated Ca^{2+} increases and rapid neuronal death after NMDA receptor activation. However, studies of cerebellar granule cells in culture suggest that oxidative damage can be a consequence (rather than a cause) of unregulated Ca^{2+} overload that follows collapse of mitochondrial membrane potential (Vesce et al., 2005; Johnson-Cadwell et al., 2007). Demands for mitochondrial ATP synthesis to handle Na^+ extrusion was suggested to be major contributor to subsequent deregulation of Ca^{2+} homeostasis in somata of these cultured neurons (Nicholls et al., 2007). It is not clear whether the relationships between energy depletion and Ca^{2+} homeostasis that have been described in neurons maintained in tissue culture also apply to neuronal preparations acutely prepared from the adult brain.

Received July 3, 2007; revised March 17, 2008; accepted March 24, 2008.

This work was supported by National Institutes of Health Grants NS 43458 and 51288. We thank Drs F. Valenzuela and W. Müller for helpful suggestions throughout the course of these experiments.

Correspondence should be addressed to Dr. C. William Shuttleworth, Department of Neurosciences, University of New Mexico School of Medicine, MSC08 4740, 1 University of New Mexico, Albuquerque, NM 87131. E-mail: bshuttleworth@salud.unm.edu.

DOI:10.1523/JNEUROSCI.5069-07.2008

 0270-6474/08/285029-11$15.00/0

When CA1 neurons acutely isolated from adult hippocampus were briefly exposed to glutamate receptor agonists, Ca^{2+} deregulation could be localized to restricted regions of apical dendrites (Connor et al., 1988; Wadman and Connor, 1992). This was demonstrated in acutely prepared hippocampal slices, in which the full dendritic arbor remains essentially intact (Connor and Cormier, 2000), and dendritic Ca^{2+} overload has been implicated as an important determinant of excitotoxic vulnerability (Shuttleworth and Connor, 2001). We recently described propagating dendritic Ca^{2+} responses in CA1 neurons after extended exposures to NMDA and found that reversal of an Na^+/Ca^{2+} exchanger did not contribute to Ca^{2+} overload (Dietz et al., 2007). The studies described here use the same NMDA model to examine whether Ca^{2+} itself is a critical causative agent for feed-forward progression of degenerative signaling and/or whether other consequences of Na^+ loading may contribute to initiation of dendritic injury.

Materials and Methods

Slice preparation. Experiments were performed in accordance with the National Institute of Health guidelines for the humane treatment of laboratory animals, and the protocol for these procedures was reviewed annually by the Institutional Animal Care and Use Committee at the University of New Mexico School of Medicine. Male FVB/N mice were obtained from Harlan (Bar Harbor, ME) at 4 weeks of age and housed under standard conditions (12 h light/dark cycle) for a maximum of 2 weeks before they were killed. Mice were deeply anesthetized with a mixture of ketamine and xylazine (85 and 15 mg/ml, respectively; 150 μl, s.c.) and decapitated. Brains were quickly removed and placed in ice-cold cutting solution containing the following (in mM): 2 KCl, 1.25 NaH_2PO_4, 6 $MgSO_4$, 26 $NaHCO_3$, 0.2 $CaCl_2$, 10 glucose, 220 sucrose, and 0.43 ketamine. Coronal sections (350 μm) were cut using a vibratome, and slices were transferred into room-temperature artificial CSF (ACSF) [in mM: 126 NaCl, 2 KCl, 1.25 NaH_2PO_4, 1 $MgSO_4$ 26 NaHCO3, 2 $CaCl_2$, and 10 glucose (equilibrated with 95%O_2/5%CO_2)]. Cutting and recording solutions were both 315–320 mOsm. After warming to 35°C and holding for 1 h, ACSF was exchanged, and slices were held at room temperature until used for recording. Individual slices were transferred to the recording chamber on a fixed-stage microscope and superfused with warmed (32°C), oxygenated ACSF at a flow rate of 2–2.5 ml/min.

Indicator loading. CA1 pyramidal neurons were visualized by using a 40× water-immersion objective on an Olympus (Tokyo, Japan) microscope (BX51WI) equipped with differential interference contrast optics. Whole-cell recordings were made by using pipettes fabricated from borosilicate glass using a horizontal pipette puller (Sutter Instruments, Novato, CA). The pipette solution contained the following (in mM): 135 K-gluconate, 8 NaCl, 1 $MgCl_2$, 10 HEPES, 2 Mg^{2+}-ATP, and 1 indicator [fura-6F, fura-2, or sodium-binding benzofuran isophthalate (SBFI)], pH 7.25 adjusted with KOH. Voltage-clamp recordings were made using a Multiclamp 700 A amplifier (Molecular Devices, Sunnyvale, CA), and cells were discarded (1) if the current required to maintain a holding voltage of −70 mV exceeded ± 100 pA or (2) if the membrane resistance was below 100 MΩ or exceeded 250 MΩ. After obtaining whole-cell access, dialysis (indicator loading) was strictly limited to 3 min. Pipettes were then slowly removed (~0.5 μm/s) while continuously monitoring membrane resistance and soma Ca^{2+} or Na^+ levels. Cells were discarded if soma Ca^{2+} or Na^+ elevations were detected. The patch pipette removal process took ~1 min to complete. Cells were then allowed to recover for 25 min after pipette removal before NMDA challenge, to allow diffusion of indicator into dendritic processes. This time was judged to be sufficient to allow equilibrium in the distal processes based on measurements of indicator concentration quite remote from somata. Reliable measurements could be made 200–250 μm from the somata and showed an initial rise in fluorescence at 0–15 min and a plateau until ~30 min. To see whether this plateau represented actual equilibration of the dendritic and not simply equal influx from the soma and efflux to more distal parts of the dendritic tree, we monitored the decrease in soma fluorescence after electrode removal. This quantity declined initially but reached a near-asymptotic value at 20–25 min, indicating that there was no (or little) outflow from the soma and that the dendritic measurement reflected equilibration or near equilibration. To further address this point, we also tested the effects of doubling the incubation time (to 40 min) and found that the characteristics of propagating dendritic Ca^{2+} signals (described below) were unchanged, still occurring with mean delay of 35–40 min and propagating from apical dendrites. We have made estimates of indicator concentration at the soma (based on fluorescence intensity comparisons with neurons extensively dialyzed with known indicator concentrations) and conclude a concentration ~200 μM, which is consistent with previous reports (Petrozzino and Connor, 1994).

Ca^{2+} and Na^+ measurements. Fluorescence measurements were made using a CCD-based system (Polychrome IV monochromator, IMAGO camera; T.I.L.L. Photonics, Pleasanton, CA). Indicators were excited at 350/380 nm, and emission was collected at 510 ± 40 nm. Image pairs were collected at 0.2 Hz. For figure presentation, images were first background subtracted, and then ratio images were generated and filtered using 3 × 3 pixel averaging. Final images were masked using an image generated from raw 380 nm fluorescence images. Conversion to Ca^{2+} concentrations was done using unfiltered pixel values, using an equation described previously (Grynkiewicz et al., 1985): $[Ca^{2+}] = K_D(R - R_{min}/R_{max} - R)(S_{f2}/S_{b2})$, where R_{min} and R_{max} are ratios at zero and saturating Ca^{2+} levels, and S_{f2}/S_{b2} is the ratio of calcium-free to calcium-bound fluorescence at 380 nm excitation. R_{min}, R_{max}, and S_{f2}/S_{b2} values were determined from calibration solutions (containing 1 mM Mg^{2+}) that were loaded into thin-walled capillary tubes to prevent quenching effects and imaged within the recording chamber with the same water-immersion objectives as used for neuronal recordings. A K_D value of 224 nM was assumed for fura-2 studies [calculated for 1 mM Mg^{2+} solutions (Grynkiewicz et al., 1985)] and 5.3 μM for fura-6F (Invitrogen, Carlsbad, CA). Because of the assumptions made in using these values, the calculated values should only be considered estimates of intracellular Ca^{2+} concentrations.

Calibration of SBFI signals was attempted but not found to be reliable in these preparations. Comparison of *in situ* ratios with *in vitro* standards (containing 135 mM K^+) showed that *in vitro* comparisons were not appropriate, because R_{max} values *in vitro* were less than maximal responses in neurons. Attempts at *in situ* calibrations (using monesin and gramicidin) were greatly complicated by substantial swelling of the slice and significant and rapid loss of 380 nm indicator signal. For these reasons, SBFI results are presented as ratio changes throughout the manuscript.

Reagents and solutions. NMDA was applied in modified ACSF lacking added Mg^{2+}. This solution was applied without preexposure to Mg^{2+}-free ACSF, so there is expected to be some delay in NMDA receptor activation attributable to the time taken to reduce extracellular Mg^{2+} concentrations from the slice. The L-type Ca^{2+} channel blocker nimodipine (10 μM) was routinely included in all solutions after indicator loading. This is similar to the use of nifedipine (10 μM) in studies of protracted NMDA exposures in cultured cerebellar granule neurons (Rego et al., 2001). In preliminary experiments, nimodipine was found to reduce somewhat the incidence of nonrecoverable initial Ca^{2+} loading in CA1 somata soon after onset of NMDA exposures. However, nimodipine did not modify the kinetics of initial or sustained Ca^{2+} overload described below ($n = 3$; data not shown). In experiments to test the effects of elevated [ATP] in the pipette solution, Mg^{2+}ATP was increased from 2 to 10 mM, which was calculated to increase free [ATP] from 0.18 to 1.03 mM [WEBMAXCLITE version 1.15 software, http://www.stanford.edu/~cpatton/maxc.html (Patton et al., 2004)].

Except when noted, all reagents were from Sigma (St. Louis, MO). Stocks of nimodipine and ifenprodil were prepared in ethanol. Stocks of NMDA and TTX (in citrate buffer) (Calbiochem, San Diego, CA) were prepared in water. RO 256981 [*R*-(*R*,*S*)-α-(4-hydroxyphenyl)-β-methyl-4-(phenylmethyl)-1-piperidine propranol] (Fischer et al., 1997) and MK-801 [(+)-5-methyl-10,11-dihydro-5*H*-dibenzo [a,d] cyclohepten-5,10-imine maleate] stocks were in DMSO. Nominally Ca^{2+}-free ACSF was prepared without added $CaCl_2$ (without added ch-

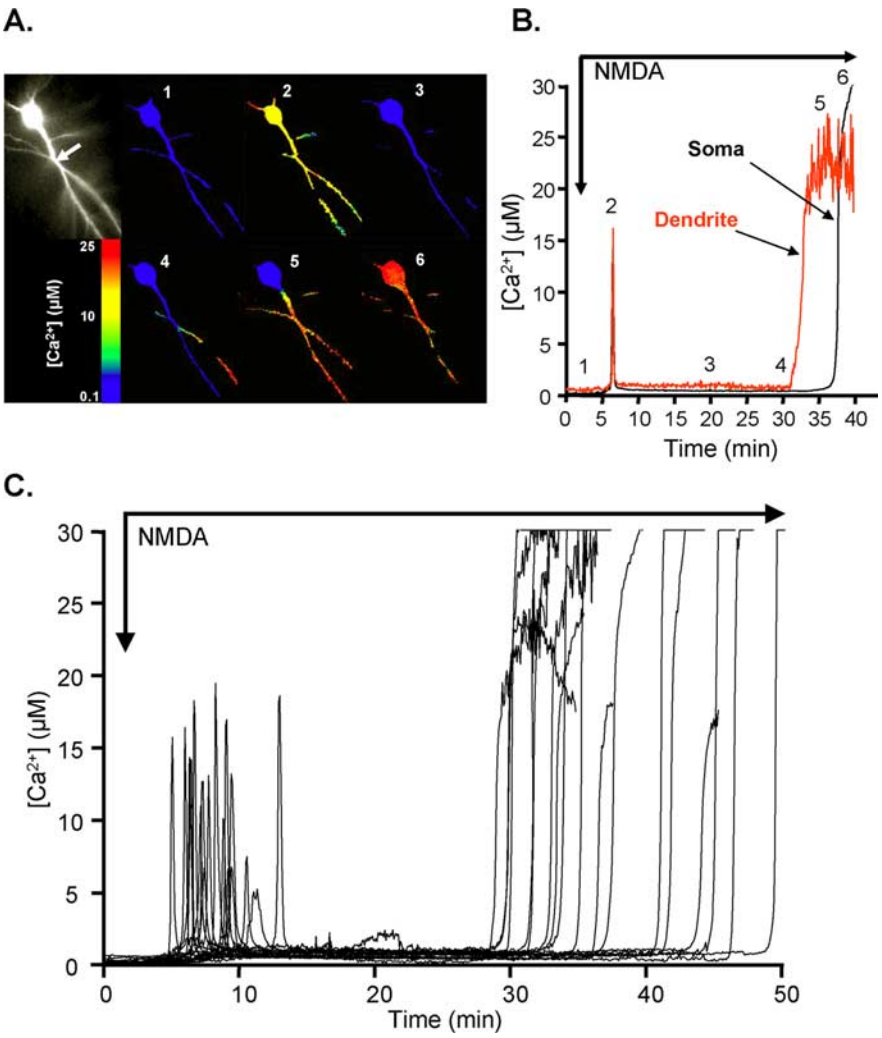

Figure 1. Propagating secondary Ca^{2+} increases, initiated in apical dendrites. ***A***, Ca^{2+} responses in a CA1 neuron during sustained exposure to NMDA. Left shows raw fura-6F fluorescence. Panels 1–6 are masked images pseudocolored to map Ca^{2+} concentration before NMDA (1) and during 40 min NMDA exposure (2–6). After an initial Ca^{2+} transient (2), the cell recovered to near-resting Ca^{2+} levels (3). After a long delay, sustained Ca^{2+} increases appeared first in a dendrite branch (4) and propagated through the entire neuron (5, 6). ***B***, Data extracted from regions of interest in the soma and dendrite (location indicated by arrow) from the neuron shown in ***A***. ***C***, Population data, showing Ca^{2+} responses recorded from somata of 18 neurons, from slices prepared from 12 animals.

elators) and resulted in free Ca^{2+} concentrations of <10 μM (Chinopoulos et al., 2007). Reduced Na^+ ACSF was prepared by supplementing 50% of NaCl with LiCl to produce a 41% reduction in total Na^+.

Results

Ca^{2+} responses in CA1 pyramidal neurons produced by NMDA

Persistent NMDA exposure (5 μM, Mg^{2+}-free ACSF; see Materials and Methods) produced a complex pattern of Ca^{2+} increases in CA1 neurons in slice (Fig. 1). An initial transient increase in cytosolic Ca^{2+} concentration ("Ca^{2+} spike") in the soma and dendrites was followed, after a long delay, by a large sustained Ca^{2+} increase ("Ca^{2+} overload") that originated in distal apical dendrites that propagated toward the soma, ultimately involving the entire neuron (Dietz et al., 2007, their Fig. 3). Because a goal of the present study was to determine the contribution of Ca^{2+} itself to the initiation and/or propagation of Ca^{2+} overload responses, the characteristics of Ca^{2+} transients were first considered here in more detail.

When measured using the low-affinity indicator fura-6F, initial Ca^{2+} spikes occurred after a delay of 6.8 ± 0.5 min after onset of NMDA exposures. The peak of these events were estimated at 12.6 ± 1.0 μM and were 16.5 ± 1.8 s in duration ($n = 18$) (Fig. 1*C*). Initial Ca^{2+} spikes were followed by substantial, but not complete, recovery of Ca^{2+} concentrations (to 0.83 ± 0.07 μM measured 5 min after each peak; $n = 18$). Some experiments were repeated with the high-affinity indicator fura-2 to more accurately assess the delay before initial Ca^{2+} spikes. Fura-2 revealed smaller Ca^{2+} oscillations (<500 nM) (Fig. 2) first detected 3.5 ± 1.0 min after NMDA exposure. These events occurred at a mean frequency of 4.0 ± 0.2/min and summated to ~1 μM before the larger transient increase (which saturated fura-2) was observed. A 10 min preexposure to Mg^{2+}-free ACSF before NMDA/Mg^{2+}-free solution greatly reduced the delay before onset of oscillations, implying that Mg^{2+} washout from the slice contributed significantly to the delay (data not shown). After recovery from the initial Ca^{2+} spike, somatic Ca^{2+} levels were estimated with fura-2 to be 264 ± 43 nM ($n = 4$). The mechanisms underlying initiation and recovery from Ca^{2+} spikes were not investigated further because these events were not required for triggering propagating sustained Ca^{2+} elevations in dendrites (see below). However, it is possible that mitochondrial Ca^{2+} accumulation and/or forward operation sodium-calcium exchanger (NCX) activity could contribute to the initial recovery of cytosolic Ca^{2+} levels.

Subsequent Ca^{2+} overload responses originated in distal apical dendrite segments. In most cases (>90%), the initiation sites were outside the field of view (>150–200 μm from somata). In the remaining neurons, there was no delay before the onset of Ca^{2+} overload, and these neurons were excluded from additional analysis. Dendritic Ca^{2+} overload responses were observed as a steep Ca^{2+} front that propagated slowly along the primary apical dendrites toward somata. These events usually were visualized first in a single branch of the apical dendritic tree, before they spread to involve all processes (Fig. 1*A*). An average propagation rate of 1.1 ± 0.2 μm/s was calculated from neurons in which an unbranched dendrite segment was fully within the plane of focus for a region of 30–80 μm from the soma (7 of 18 neurons). On average, sustained Ca^{2+} increases reached the soma 28.5 ± 1.5 min after the initial Ca^{2+} spike in each neuron ($n = 18$). The average total time taken for Ca^{2+} overload responses to arrive at the soma (after onset of NMDA exposure) was 35.3 ± 1.5 min (range, 27.7–48.1 min; $n = 18$) (Fig. 1*C*). The range may be contributed to, in part, by nonuniform propagation rates along branched dendrites and/or differences in the location of initiation sites of dendritic Ca^{2+} deregulation.

Sustained Ca^{2+} increases were persistent and ultimately were sufficient to saturate the indicator in most cases (estimated at

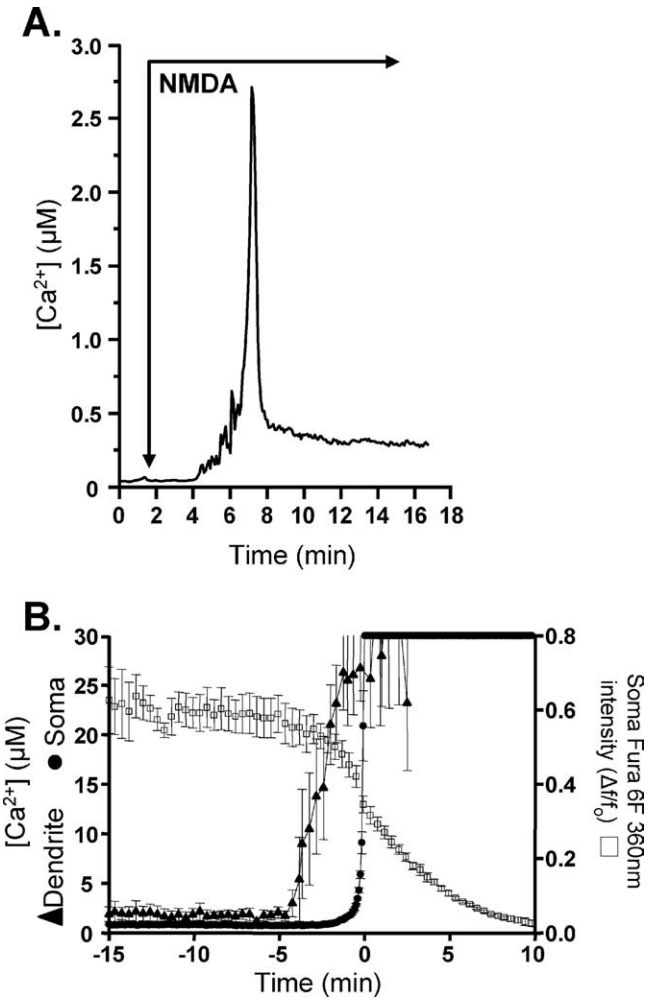

Figure 2. ***A***, The higher-affinity Ca^{2+} indicator fura-2 revealed initial Ca^{2+} oscillations. In this representative example from a fura-2-loaded neuron, small Ca^{2+} oscillations were observed soon after the onset of NMDA exposure. Individual small events summed together before a single much larger transient was triggered. The initial Ca^{2+} oscillations seen here were too small to be reliably detected in the other figures in which the lower-affinity indicator fura-6F was used. ***B***, Rapid indicator loss after establishment of sustained Ca^{2+} increases in somata. Sustained Ca^{2+} increases are shown for regions in the proximal apical dendrite (50–75 μm from somata; triangles) and within somata (circles), during persistent NMDA exposures. Records have been aligned to the onset of sustained somatic Ca^{2+} elevations in each neuron. Indicator levels were monitored in somata at the isobestic point for fura-6F (360 nm; squares, relative to levels after initial loading) and showed prompt decreases after the arrival of sustained Ca^{2+} increases. All data represent mean ± SEM from five neurons.

>30 μM; see Materials and Methods). After invasion of somata, sustained Ca^{2+} increases were accompanied by prompt indicator loss (Fig. 2*B*), suggesting significant compromise of membrane integrity (Randall and Thayer, 1992; Avignone et al., 2005).

In the current study, we concentrated our analysis on signals in apical dendrites, because, in every case using extended NMDA exposure, neuronal injury (loss of somatic Ca^{2+} homeostasis and loss of indicator) did not occur until the arrival of sustained Ca^{2+} increases from the apical dendrite. However, there were a small number of cases (5 of 25 in a sample of control neurons) in which a segment of basal dendrite close to the soma did demonstrate Ca^{2+} elevations during NMDA exposure. These basal dendrite responses sometimes remained elevated for 20–30 min before sustained Ca^{2+} elevations were noted in apical dendrites but never themselves progressed into somata and triggered degeneration. A similar small proportion of basal dendrite signals was also noted in a previous study with NMDA stimulation (2 of 22 neurons tested). This contrasted with responses to inhibition of Na^+/K^+/ATPase activity with ouabain, in which responses invariably initiated in basal dendrites and invaded somata (Dietz et al., 2007). As discussed previously, differences in NMDA receptor distribution between apical and basal dendrites could contribute to these differences between responses to NMDA and ouabain (Dietz et al., 2007). In addition, ATP depletion is not expected during ouabain exposure, in contrast to the effects of NMDA stimulation (see below).

Effects of transient Ca^{2+} removal on arrival of propagating dendritic Ca^{2+} increases at somata

We tested the hypothesis that Ca^{2+} accumulation was required for feedforward propagation of Ca^{2+} overload along dendrites under this stimulus protocol. In the first set of experiments, the initial Ca^{2+} spike was allowed to develop, and then extracellular Ca^{2+} was transiently washed out. If Ca^{2+} influx is required for the propagation of Ca^{2+} overload responses along dendritic process, we reasoned that transient removal (10 or 20 min) of extracellular Ca^{2+} (see Materials and Methods) should result in a corresponding delay in arrival of overload Ca^{2+} responses at somata, after restoration of extracellular Ca^{2+} concentration to 2 mM.

Figure 3*A* shows that, when Ca^{2+} was removed for 10 min immediately after initial Ca^{2+} transients, there was no significant delay in the arrival of the Ca^{2+} overload (interval between initial Ca^{2+} spike and arrival of response at somata; 27.8 ± 1.9 min control and 27.2 ± 3.8 with Ca^{2+} removal; $p = 0.87$). In separate interleaved experiments, longer periods of transient Ca^{2+} washout also did not result in a significant delay in the interval between initial and sustained Ca^{2+} (10 min washout 31.3 ± 2.9 min vs 20 min washout 29.6 ± 1.95; $p = 0.64$; $n = 7$ each).

Figure 3*B* shows results from a second set of experiments, from which we found that the initial Ca^{2+} spikes were not required for initiation of the Ca^{2+} overload responses in dendrites. Extracellular Ca^{2+} was removed for 10 min before NMDA application and Ca^{2+}-free media was continued for an additional 10 min ($n = 6$) (as illustrated in Fig. 3*B*) or 20 min ($n = 6$) after initiation of NMDA exposure. In each case, there was no Ca^{2+} spike, implying that its generation was dependent on Ca^{2+} influx. In addition, there was not a detectable increase in somatic or dendritic Ca^{2+} after reintroduction of 2 mM Ca^{2+} ACSF. In every case, the prevention of initial Ca^{2+} spikes did not prevent the subsequent initiation and propagation of sustained Ca^{2+} increases along apical dendrites. Furthermore, the duration of Ca^{2+} removal did not significantly affect the mean arrival time of sustained Ca^{2+} increases at somata (measured from onset of NMDA exposure), consistent with the results described above (33.3 ± 1.93 vs 37.9 ± 2.2 min; 20 and 30 min total Ca^{2+} washout time, respectively; $p = 0.16$; $n = 6$ each). These values are very close to those described above for control responses in which 2 mM Ca^{2+} was maintained throughout the experiment (35.3 ± 1.5 min) (described above for Fig. 1*C*).

These results suggested that sustained Ca^{2+} increases in dendrites may simply report the location of a propagating degenerative response rather than being a required agent for feedforward of ionic deregulation along CA1 dendrites.

Effects of protracted Ca^{2+} removal

Much longer periods of Ca^{2+} removal supported the idea that Ca^{2+} was not required for progression of degeneration along dendrites but also suggested that Ca^{2+} overload was required for

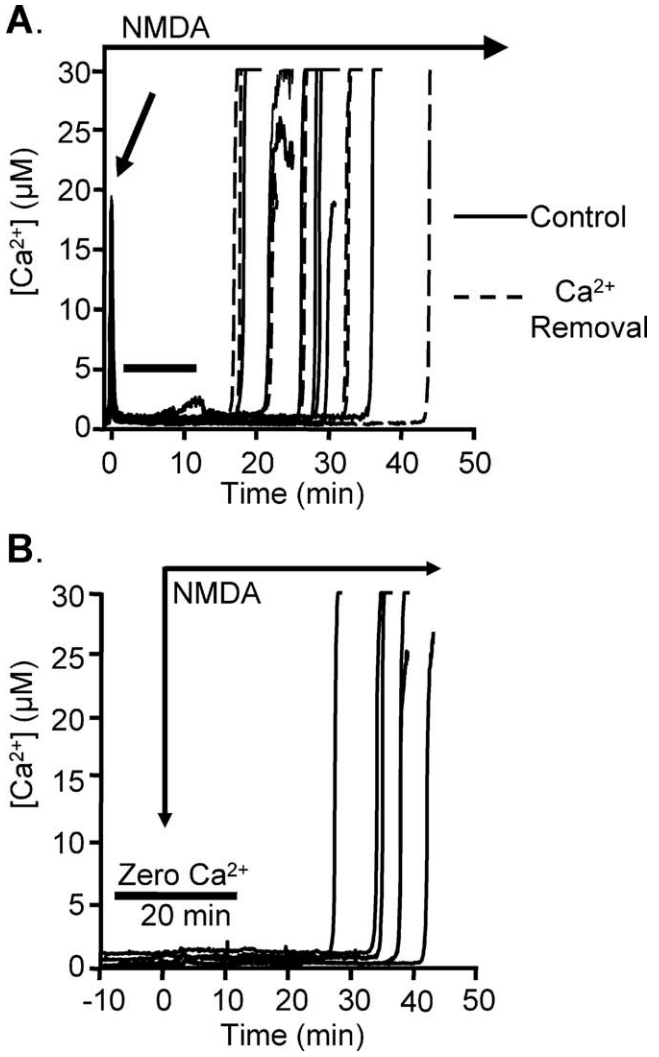

Figure 3. ***A***, Lack of effect of transient Ca^{2+} removal on the progression of subsequent Ca^{2+} overload. Soma Ca^{2+} levels (measured with fura-6F) from neurons exposed to NMDA. NMDA was present throughout all recordings, and initial Ca^{2+} transients have been aligned for all neurons at the 0 min time point (arrow). In seven experiments (dashed lines), the superfusate was switched to Ca^{2+}-free ACSF for 10 min (horizontal bar) after the initial Ca^{2+} transient. Ca^{2+} was then restored to 2 mM, and sustained Ca^{2+} increases were monitored. These experiments were interleaved with seven experiments in which 2 mM Ca^{2+} was maintained throughout NMDA exposures (solid lines), and the two datasets showed overlapping ranges of responses. ***B***, Preventing initial Ca^{2+} transients did not delay subsequent Ca^{2+} overload. Slices were superfused with Ca^{2+}-free ACSF for 20 min, beginning 10 min before onset of NMDA exposure. Initial Ca^{2+} transients were not observed, but, after restoration of extracellular Ca^{2+}, sustained Ca^{2+} overloads still reliably propagated from apical dendrites to somata. The overall delay in overload responses was similar to responses in Figure 3*A*, but note that intervals are measured here from the onset of NMDA exposure to the time of arrival of Ca^{2+} overload at somata (rather than between initial Ca^{2+} transients and Ca^{2+} overload in Fig. 3*A*). Six neurons from five animals; fura-6F was used throughout.

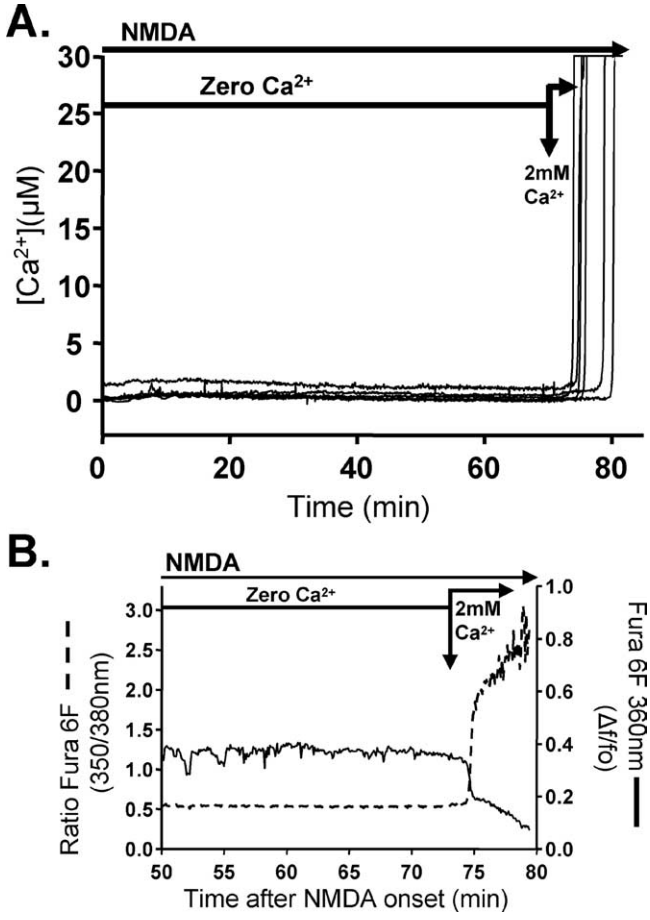

Figure 4. Effects of protracted Ca^{2+} removal. ***A***, Each trace shows the somatic Ca^{2+} levels in a fura-6F-loaded neuron. Extracellular Ca^{2+} was washed out 10 min before the start of NMDA and then withheld for an additional 70 min of NMDA exposure (5 μM). After reintroduction of 2 mM Ca^{2+}, all six neurons showed prompt and rapid dendritic Ca^{2+} increases that progressed almost immediately into somata. ***B***, Somatic fura-6F levels (measured at 360 nm) were well maintained throughout the protracted NMDA exposure in Ca^{2+}-free ACSF but decreased dramatically after reintroduction of 2 mM Ca^{2+}. This representative example shows the coincident decrease in 360 nm fluorescence (solid line) as somatic Ca^{2+} levels rise to very high levels (dashed line).

ultimate loss of membrane integrity. Extracellular Ca^{2+} was washed out for 10 min period before NMDA onset and was withheld for an additional 70 min of NMDA exposure. In nominally Ca^{2+}-free ACSF, progressive dendritic Ca^{2+} increases were never observed. However, after reintroduction of 2 mM Ca^{2+}, all six neurons showed prompt and rapid dendritic Ca^{2+} increases that appeared in multiple dendritic processes almost immediately after reestablishment of Ca^{2+} levels in the recording chamber. The propagation rate of sustained Ca^{2+} elevations along the proximal apical dendrite was approximately threefold faster than in control conditions (3.1 ± 0.9 μm/s; $n = 4$) and had fully involved the somata within 3.5 ± 0.9 min after Ca^{2+} had reached the recording chamber (Fig. 4*A*).

Throughout this time course, there was no evidence of membrane compromise in neuronal somata, because indicator fluorescence (monitored at 360 nm) in single loaded neurons remained stable during the entire 70 min 0-Ca^{2+} NMDA period (Fig. 4*B*). However, indicator levels promptly declined after Ca^{2+} was reintroduced and somatic Ca^{2+} elevations were elevated to sustained high levels. These results suggest that Ca^{2+}-independent mechanisms underlie progression of degenerative signaling along dendrites but that Ca^{2+} elevations are required for ultimate neuronal demise.

Intracellular Na^+ increases resulting from persistent NMDA exposure

In contrast to the compound Ca^{2+} responses, NMDA produced monotonic increases in intracellular Na^+ levels (Fig. 5). The characteristics of intracellular Na^+ increases were investigated using the ratiometric indicator SBFI. Because attempts to calibrate these signals in slices were not successful, the results are

presented as SBFI ratio changes (see Materials and Methods). NMDA produced mean SBFI ratios increases of 0.99 ± 0.06 (n = 11) that reached half-maximal levels 5.4 ± 0.7 min after NMDA onset (90% peak at 7.3 ± 0.7 min). As shown in Figure 5*C*, SBFI ratios did not show any significant recovery toward baseline levels throughout the NMDA exposures, in contrast to the prompt recovery of initial Ca^{2+} transients (Fig. 1).

Effects of NMDA receptor block on Ca^{2+} and Na^+ elevations

We examined whether continuous NMDA receptor activation was required for the events described above. An alternative possibility is that transient NMDA receptor stimulation might be sufficient to set in motion a chain of events that ultimately resulted in delayed Ca^{2+} overload.

In the first set of studies, the open-channel NMDA receptor blocker MK-801 (50 μM) was applied immediately after initial Ca^{2+} transients. In no case was a sustained Ca^{2+} increase observed in apical dendrites or somata (monitored for 60 min) (Fig. 6*A*). When applied 10 min after onset of NMDA exposure, MK-801 caused SBFI ratios to promptly return toward basal levels (5.6 ± 1.1 min to 90% recovery to prestimulus levels; n = 6) (Fig. 6*B*). These results suggest that persistent NMDA receptor activation was required to maintain sustained Na^+ elevations and delayed sustained Ca^{2+} elevations.

MK-801 also reversed sustained Ca^{2+} increases that had already been established in proximal locations of dendrites. MK-801 was applied rapidly to the slice after a sustained dendritic Ca^{2+} response was visualized. In four of five neurons tested, Ca^{2+} returned promptly to near-basal intracellular Ca^{2+} concentrations (Fig. 7). In one of the neurons, the response was halted temporarily before the response progressed very slowly into the soma.

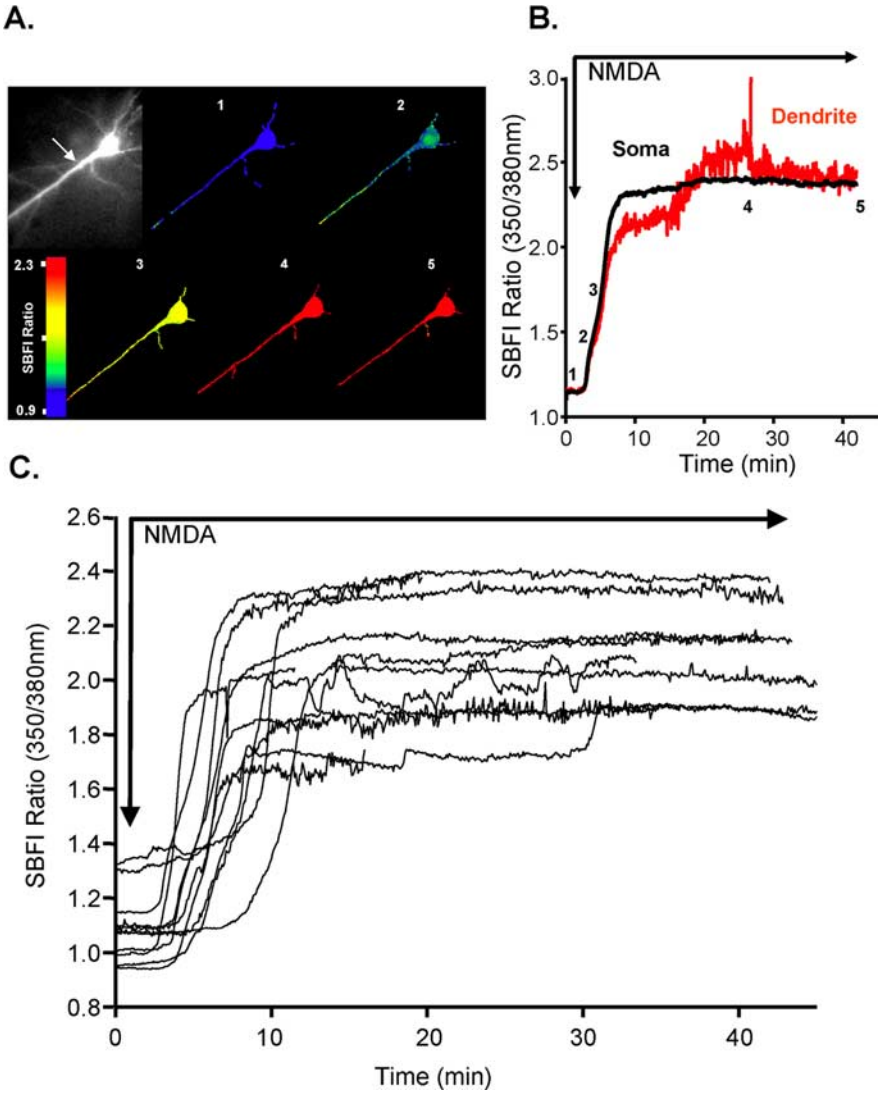

Figure 5. Intracellular Na^+ increases. ***A***, Responses of the Na^+-sensitive indicator SBFI in a CA1 neuron during sustained exposure to NMDA. Left shows raw SBFI fluorescence. Panels 1–5 are masked images pseudocolored to map SBFI fluorescence ratio changes (350/380 nm excitation) before NMDA (1) and during 40 min NMDA exposure (2–5). ***B***, Data extracted from two regions of interest (soma and dendrite, the latter indicated by the arrow in the left image). ***C***, Population data showing somatic responses from 11 neurons, from slices prepared from five animals.

Figure 8 shows that NR2B-containing NMDA receptors do not appear to be a major factor in the responses studied here with sustained NMDA receptor activation. NR2B-containing receptors are sensitive to inhibition by ifenprodil (Williams, 1993) and RO 256981 (Fischer et al., 1997) and have been suggested to contribute preferentially to excitotoxic injury (Liu et al., 2007). Preexposure to ifenprodil (10 μM) for 10 min before NMDA exposure did not prevent initiation and/or propagation of Ca^{2+} elevations. The total time taken (after NMDA onset) for arrival of Ca^{2+} overload responses at somata in the presence of 10 μM ifenprodil were 31.9 ± 1.6 min (n = 6), a value similar to controls (Fig. 1*C*). Na^+ elevations were not obviously modified by either RO 256981 or ifenprodil. Figure 8*B* shows that (in contrast to the actions of MK-801) ifenprodil or RO 256981 did not reverse SBFI ratios, once they had been established by NMDA exposures. In addition, preexposure to both antagonists did not modify initial SBFI ratio increases (data not shown).

Although bath application of NMDA might indirectly activate neurons throughout the slice, indirect excitation does not appear to be a significant contributor to Ca^{2+} and Na^+ dynamics in CA1 neurons recorded here. Preexposure of slices to TTX (1 μM) had little influence on Ca^{2+} responses. Initial Ca^{2+} spikes were still observed 5.9 ± 0.5 min after onset of NMDA exposure; Ca^{2+} overload responses originated in apical dendrites and arrived at somata 35.8 ± 3.6 min (n = 6). These characteristics are similar to those described for NMDA in ACSF (Fig. 1). Likewise, TTX did not alter the Na^+ dynamics when compared with controls. The delay to half-maximal Na^+ increase for TTX was 5.9 ± 0.7 min (n = 6), and the peak ratio change was 0.98 ± 0.03 (compared with delay of 5.4 ± 0.7 min and ratio change of 0.99 ± 0.06 in control conditions; see above). The noncompetitive AMPA channel blocker GYKI 53655 [1-(4-aminophenyl)-3-methylcarbamyl-4-methyl7,8-methylenedioxy-3,4-dihydro-5*H*-2,3-benzodiazepine] (50 μM) (Wilding and Huettner, 1995) did not significantly modify the amplitude of initial transient Ca^{2+} increases (21.8 ± 1.7 vs 16.4 ± 1.7 μM for control and GYKI

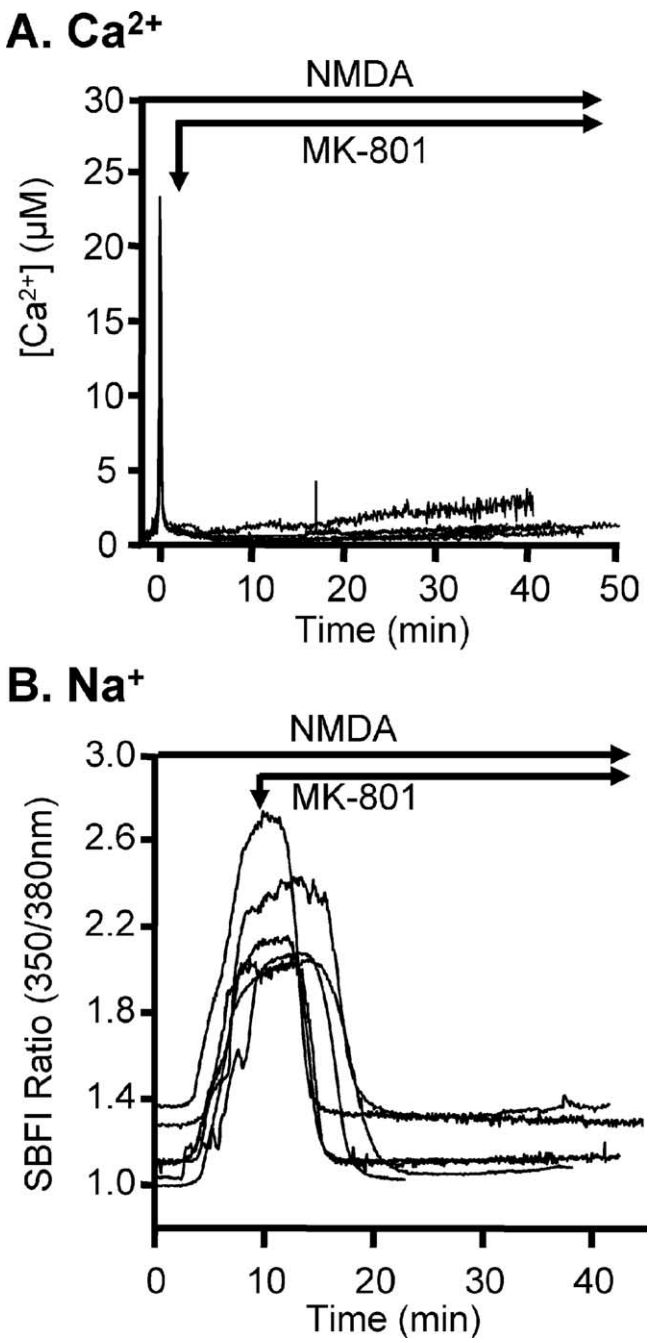

Figure 6. Effects of MK-801, applied before the development of sustained Ca^{2+} responses. ***A***, Fura-6F experiments; NMDA was present throughout, and the noncompetitive receptor antagonist MK-801 (50 μM) was timed to arrive immediately after initial Ca^{2+} increases. Initial Ca^{2+} increases for all preparations have been aligned in the figure to the 0 min time point. MK-801 prevented the development of secondary Ca^{2+} responses in all neurons tested ($n = 6$). ***B***, SBFI experiments, in which MK-801 was applied 10 min after the onset of exposure to NMDA. MK-801 promptly restored intracellular SBFI ratios to prestimulus levels in each neuron tested ($n = 6$).

53655, respectively; $n = 4$ each; $p = 0.07$) or the delay in arrival of Ca^{2+} overload at somata (40.0 ± 13.4 vs 40.1 ± 2.5 min for control and interleaved GYKI 53655 experiments, respectively; $n = 4$; $p = 0.9$). These results suggest that persistent, direct excitation of NMDA receptors on CA1 neurons is the most likely cause of the persistent Na^+ influx and Ca^{2+} deregulation described above.

Reducing extracellular Na^+ delayed progression of dendritic Ca^{2+} elevations

We tested whether Na^+ influx contributed to progressive Ca^{2+} elevation in dendrites. Responses in control ACSF with interleaved slices exposed to modified ACSF in which extracellular Na^+ was reduced to 59% of control concentrations (using LiCl as a surrogate; see Materials and Methods). Li^+ permeates NMDA receptors less well than Na^+ (Yamaguchi and Ohmori, 1990) and is also a poorer substrate of Na^+/K^+/ATPase activity than is Na^+ (Kang et al., 2004). In reduced Na^+ conditions, the initial Ca^{2+} spike was smaller (3.0 ± 0.5 μM) than in controls (10.5 ± 3.3; $p < 0.05$; $n = 6$ each). In the control set, Ca^{2+} overload was observed in somata 43.2 ± 3.2 min ($n = 6$) after onset of NMDA exposure. In reduced Na^+ ACSF, one neuron showed an unusually early sustained Ca^{2+} response (at 27.6 min), but the remaining five of six neurons showed no sign of dendritic Ca^{2+} overload, even when monitored for 60 min of NMDA exposure.

Effects of increased metabolic capacity on dendritic Ca^{2+} increase response

Extrusion of Na^+ by Na^+/K^+/ATPase activity is a major consumer of neuronal ATP (Attwell and Laughlin, 2001). We tested the possibility that delayed Ca^{2+} overload is a consequence of ATP depletion, which follows from the metabolic demand of sustained Na^+ extrusion. This was done by increasing ATP levels in the loading pipette or supplementing the superfusate with pyruvate.

Simply supplementing the pipette intracellular solution with additional ATP (10 mM rather than 2 mM added; see Materials and Methods) was sufficient to significantly delay the onset of Ca^{2+} overload responses in dendrites. As shown in Figure 9*A*, elevated intracellular ATP did not delay the initial Ca^{2+} spike but significantly decreased the amplitude (25.0 ± 3.6 vs 9.8 ± 2.8 μM for control and elevated ATP, respectively; $n = 6$ each; $p < 0.008$). The delay in Ca^{2+} overload was increased compared with control (36.5 ± 1.5 vs 57.9 ± 1.5 min for control and elevated ATP, respectively; $n = 6$ each; $p < 0.01$). Once initiated, there was no significant decrease in the rate of propagation of Ca^{2+} overload along apical dendrites (0.82 ± 0.16 vs 0.93 ± 0.25 μm/s for control and elevated ATP, respectively; $n = 6$ and 5; $p = 0.6$).

In the second set of studies (Fig. 9*B*), slices were preexposed to pyruvate (10 mM in otherwise normal ACSF) for 15 min before the onset of NMDA exposure and maintained throughout the NMDA exposure. Pyruvate reduced the rate NMDA-stimulated SBFI ratio increases (0.32 ± 0.03 vs 0.17 ± 0.04 units/s; $n = 5$; $p < 0.0017$) and caused a small reduction in the peak ratio change (ΔRatio, 1.05 ± 0.04 vs 0.93 ± 0.02 for control and pyruvate, respectively; $n = 5$ each; $p < 0.04$). Pyruvate preexposure greatly decreased the mean amplitude of initial Ca^{2+} transients (from 16.1 ± 2.9 to 1.7 ± 0.4 μM; $n = 6$; $p < 0.001$). In addition, in three of six neurons tested, no evidence of subsequent dendritic Ca^{2+} overload was observed with observation times up to 70 min. In three of six neurons tested, dendritic Ca^{2+} overload was observed but was delayed compared with five of six responses in untreated slices (mean delay of 58.3 ± 6.8 min for three responders in pyruvate vs 43.1 ± 3.2 min for interleaved controls; $n = 6$).

Discussion

This study examines mechanisms by which protracted exposure to NMDA initiates severe Ca^{2+} increases in apical dendrites of CA1 neurons, which propagate slowly throughout the neuron. We conclude that Ca^{2+} accumulation itself is not required for the initiation or progression of disrupted ionic homeostasis during

this type of agonist exposure. The initial Ca^{2+} spike was not necessary for the initiation of subsequent Ca^{2+} overload (Fig. 3), and, when the effects of transient Ca^{2+} removal were tested, it was found that the final, catastrophic somatic Ca^{2+} increase was not delayed to any significant extent (Fig. 3). In contrast to Ca^{2+} elevations, Na^+ accumulation was persistent in somatic and dendritic compartments, and extracellular Na^+ reductions delayed or prevented the propagation of dendritic Ca^{2+} increases. Furthermore, results obtained with ATP or pyruvate supplementation are consistent with the hypothesis that metabolic consequences of Na^+ loading may underlie progressive regional metabolic dysfunction and consequent Ca^{2+} overload.

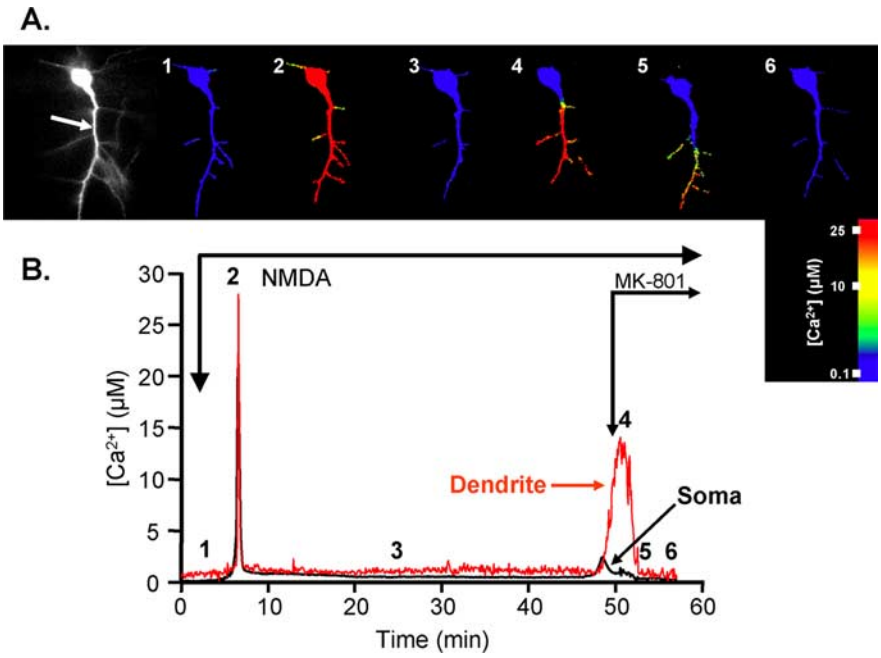

Figure 7. MK-801 was still effective when applied after the establishment of Ca^{2+} overload in an apical dendrite. This example is representative of four trials in which a sustained Ca^{2+} response was allowed to propagate along the primary apical dendrite before MK-801 (50 μM) was applied. NMDA was present throughout. ***A***, Raw fluorescence image of the neuron (left) and pseudocolor images (1–6) showing progression of a sustained Ca^{2+} response along the apical dendrite. MK-801 was applied as the sustained Ca^{2+} response advanced almost to the soma (4) and resulted in complete retraction of the response from all dendritic processes. ***B***, Extracted Ca^{2+} concentrations from a somatic region (black) and a region of dendrite (red) at the site indicated by the arrow in ***A***. Numbers correspond to panels illustrated in ***A***.

Na^+ loading

In contrast to Ca^{2+} elevations, Na^+ accumulation was monotonic and nearly contemporaneous in somatic and dendritic compartments. Previous work examining glutamate- or NMDA-induced Na^+ increases in cultured neurons have reported stable Na^+ increases ranging from 45 to 80 mM (Kiedrowski et al., 1994; Pinelis et al., 1994). The ratiometric Na^+ measurements made in the present study could not be reliably calibrated (see Materials and Methods), but it is likely that similar values are achieved here.

The major route of Na^+ entry was via NMDA receptors on CA1 neurons. SBFI ratio increases were promptly reversed by MK-801, and, from the lack of effect of TTX and GYKI 53655, it appears that other ionotropic glutamate receptors and voltage-gated Na^+ channels made little direct contribution. NR2B-containing NMDA receptors have been implicated in other studies of excitotoxic injury (Reyes et al., 1998; Liu et al., 2007), but antagonists selective for NR2B NMDA receptors were without effect on Na^+ or Ca^{2+} dynamics (Fig. 8). It is suggested that the contribution of NR2B receptor mechanisms to NMDA-mediated toxicity is quite low in slices from adult animals [when compared with neonatal tissue (Zhou and Baudry, 2006)], and this developmental change may explain the lack of NR2B contribution here.

Mechanisms coupling sustained Na^+ loads to dendritic Ca^{2+} increases

Among the several possible outcomes of extended intracellular Na^+ elevation, demands of increased Na^+/K^+/ATPase activity is a critical consequence (Chinopoulos et al., 2000; Greenwood et al., 2007), and our results appear consistent with the idea that ATP depletion is a major mechanism underlying the ultimate loss of Ca^{2+} homeostasis. Increasing the concentration of ATP in the dialysis pipette significantly delayed the arrival of dendritic Ca^{2+} increases at the soma (Fig. 9*A*), and supplying exogenous pyruvate provided sufficient additional metabolic competence to delay or even prevent the loss of Ca^{2+} regulation (Fig. 9*B*). Importantly, Na^+ loading was not greatly decreased during pyruvate exposures, suggesting that ATP depletion is downstream of Na^+ loading rather than the bulk of the Na^+ increase resulting from a progressive loss of ATP-dependent extrusion. Intracellular Ca^{2+} levels are expected to rise dramatically if ATP-dependent Ca^{2+} extrusion and sequestration mechanisms become compromised in the face of heightened Ca^{2+} influx through NMDA receptors. Progressive failure of Na^+/K^+/ATPase activity would also be expected, and we have shown previously that direct inhibition of Na^+/K^+/ATPase with ouabain can produce dendritic Ca^{2+} deregulation (Dietz et al., 2007). The reason why supplementation with either ATP or pyruvate is effective here, despite the continual superfusion of slices with 10 mM glucose, is currently unknown. It is possible that neuronal glucose transport becomes limiting, and/or glial-neuronal metabolic coupling is insufficient under these stimulation conditions.

Cytosolic Na^+ loading can also drive cytosolic Ca^{2+} elevations more directly, as a consequence of Na^+/Ca^{2+} exchange at the plasma membrane (Kiedrowski, 2007) and mitochondrial inner membrane (Hoyt et al., 1998b). Although it is possible that exchange at both sites contributes to Ca^{2+} overload measured here, we showed recently that an inhibitor selective for the reverse-operation mode of plasma membrane NCX1–NCX3 isoforms did not influence dendritic Ca^{2+} overload responses to NMDA under very similar circumstances, suggesting little contribution from plasma membrane Na^+-dependent NCX reversal with this particular stimulus (Dietz et al., 2007). Na^+ loading and activation of mitochondrial $2Na^+/Ca^{2+}$ exchange contributes to somatic Ca^{2+} elevations during oxygen and glucose removal from hippocampal slices (Zhang and Lipton, 1999) (see also Scanlon et al., 2000). A similar exchange may contribute to initial Ca^{2+} transients observed here, but it might be expected that mitochondrial Ca^{2+} capacity would be progressively drained by this pathway during sustained Na^+ elevations (Hoyt et al., 1998a) and thus not be able to contribute significantly directly to the

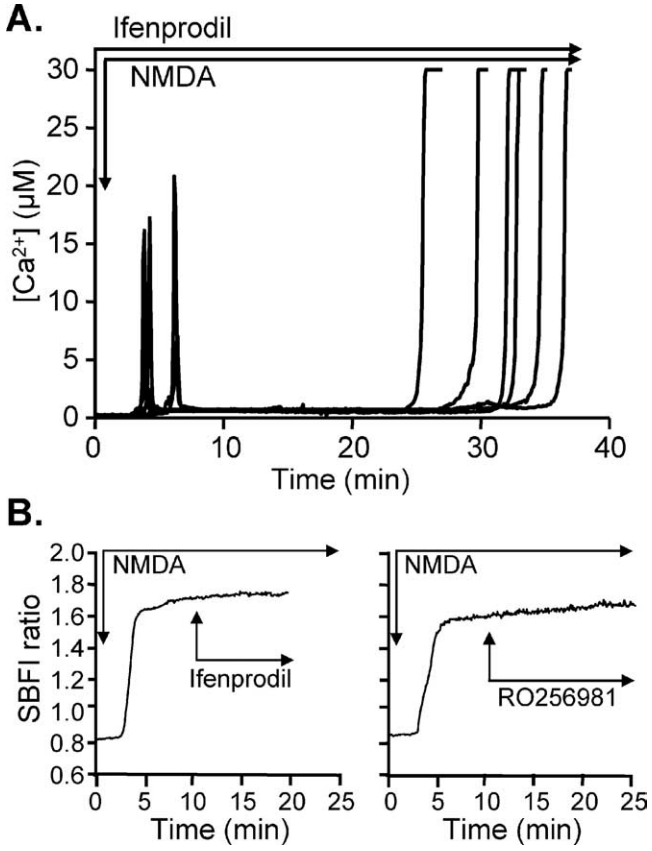

Figure 8. Lack of effect of antagonists with selectivity for NMDA receptors containing NR2B subunits. ***A***, Slices were preexposed to ifenprodil (10 μM) for 10 min before onset of NMDA exposure and remained present throughout. Ca^{2+} dynamics (somatic fura-6F measurements shown here) were similar to control responses described above (see Fig. 1), with initial Ca^{2+} transients followed by sustained Ca^{2+} overloads that initiated in apical dendrites before propagating to produce sustained somatic Ca^{2+} elevations. ***B***, Representative examples showing that exposure to either ifenprodil (10 μM; left) or RO 256981 (10 μM; right) did not reverse Na^+ elevations that had been established by NMDA exposures. SBFI ratios were measured in somatic compartments.

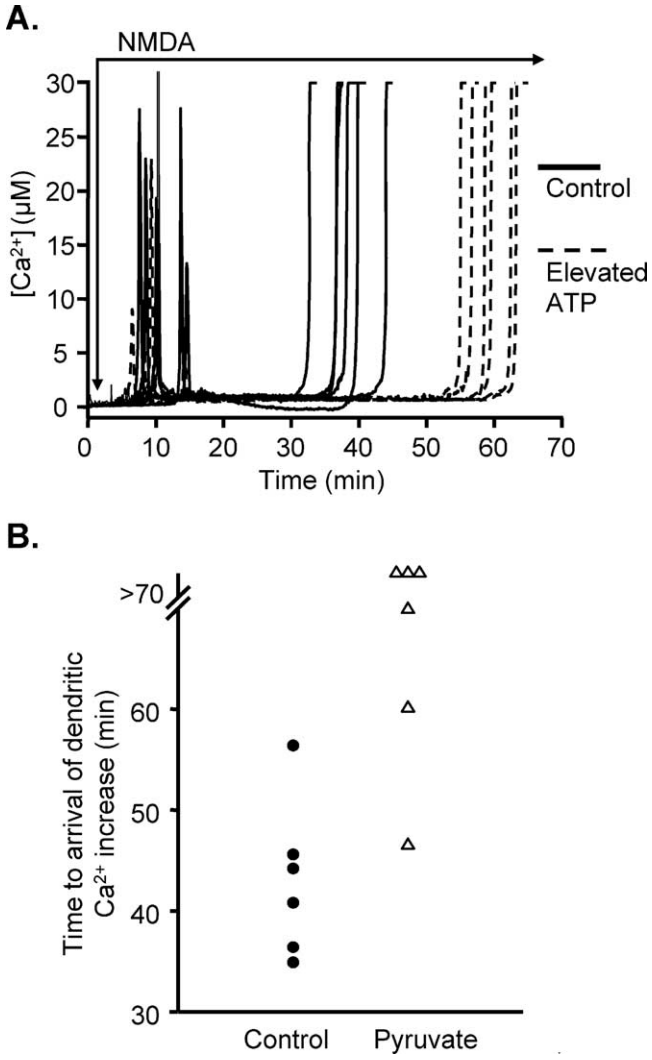

Figure 9. ***A***, Increasing ATP concentration in the loading pipette delayed propagation of dendritic Ca^{2+} overload to somata. Solid lines show responses to NMDA exposure in neurons loaded for 3 min with fura-6F, in standard intracellular solution (2 mM added ATP; solid lines) (see Results). These experiments were interleaved with experiments in which 10 mM ATP was added to the intracellular loading solution (dashed lines). All other experimental conditions were unchanged. This manipulation did not change the average time to onset of the initial Ca^{2+} increases but significantly increased the time taken for sustained Ca^{2+} overload responses to arrive from apical dendrites to somata. ***B***, Supplementation of ACSF with pyruvate prevented or delayed propagation of dendritic Ca^{2+} overload to somata. Each symbol represents the time taken for a Ca^{2+} overload response to arrive at the soma in a single preparation, after onset of exposure to NMDA. Filled circles show responses when slices were challenged in standard ACSF (10 mM glucose), as shown above (see Fig. 1). These experiments were interleaved with slices superfused with modified ACSF containing 10 mM pyruvate plus 10 mM glucose (20 min preexposure and maintained throughout NMDA challenge, indicated by triangles). Three of the pyruvate-supplemented preparations did not show any dendritic Ca^{2+} overload within the 70 min observation period. Ca^{2+} overload was observed in the other three pyruvate-supplemented preparations but occurred later than was seen in five of six of the matched control preparations.

delayed Ca^{2+} overload. The relative contribution of these pathways, together with metabolic depletion, remains to be determined.

Relationship to previous studies of progressive calcium deregulation in dendrites

It is noted that the slowly propagating Ca^{2+} overload described here is quite similar in appearance to a previously reported phenomenon in dendrites of adult hippocampal neurons, termed a "secondary Ca^{2+} response" (Connor et al., 1988; Wadman and Connor, 1992; Connor and Cormier, 2000; Shuttleworth and Connor, 2001). Both responses first appear in distal dendrites before slowly invading the rest of the neuron, but, despite the similarities, key differences suggest that different underlying mechanisms are involved. First, initiation of the "secondary response" was accomplished by multiple, relatively brief exposures to an excitatory amino acid, and, after establishment of the secondary response, no additional exposure to the agonist was required and glutamate receptor antagonists were ineffective in reversing it (Connor et al., 1988; Wadman and Connor, 1992). In the present example, persistent NMDA exposure was required, and MK-801 was immediately effective in reversing the response (Fig. 7). Second, secondary Ca^{2+} responses were triggered by repeated Ca^{2+} overloads, which then set in motion a feedforward progression of Ca^{2+} deregulation along the dendrite. In this study, there was no requirement at all for an initial Ca^{2+} spike to initiate a delayed dendritic Ca^{2+} overload (Fig. 3). The model used here depends on continuous receptor activation, which presumably causes a progressive metabolic crisis attributable to Na^+ influx, occurring first in the smallest apical dendritic compartments and ending in the mitochondria-rich somata. It seems

likely that a rich NMDA receptor distribution, together with large surface area/volume ratios of small apical dendrites combine to cause large local demands on ATP production. However, it is also possible that events initiate in remote dendritic processes attributable to a relative lack of ATP-generating machinery at these sites.

Similar mechanistic differences may contribute to the diversity of responses seen after glutamate receptor stimulation in neuronal cultures. For example, in many studies of cultured hippocampal or cortical neurons, brief exposures to glutamate receptor agonists triggers a large initial cytosolic Ca^{2+} increase required for delayed toxicity (Randall and Thayer, 1992). A cascade of deleterious effects can be triggered by a brief period of mitochondrial Ca^{2+} loading (Stout et al., 1998) and then proceeds without receptor activation. Brief exposures of cultured rat hippocampal neurons to high concentrations of glutamate lead to very large sustained inward current and Ca^{2+} influx that persist after glutamate removal (Deshpande et al., 2007) (see also Chen et al., 1997). This current appears to be mediated by a novel Ca^{2+}-permeable Gd^{3+}-sensitive current (Deshpande et al., 2007). It seems possible that such mechanisms could contribute to the secondary Ca^{2+} responses seen in dendrites after brief intense receptor stimulation but not the responses seen here (because MK-801 effectively blocked Ca^{2+} elevations).

Something more akin to the present work may be seen in some studies of cultured cerebellar granule neurons. Glutamate exposures resulted in collapse of the ATP/ADP ratio (Budd and Nicholls, 1996) and ATP deficiencies were suggested to be important initiators for subsequent uncontrolled Ca^{2+} increases (Brocard et al., 2001; Jekabsons and Nicholls, 2004). Interestingly, if NMDA receptor-mediated influx was terminated with MK-801, somatic Ca^{2+} deregulation was prevented in some neurons, but other neurons within the same cultures still underwent deregulation (Castilho et al., 1998). It was proposed that MK-801 was not protective if somata of neurons were about to deregulate or had already done so (Castilho et al., 1998). It would be interesting to know whether the window for protection is related to the propagation of events from dendritic initiation sites to somata. Although localized Ca^{2+} overload has been identified in dendrites in culture after glutamate receptor stimulation (Randall and Thayer, 1992; Bindokas and Miller, 1995), the idea that dendritic Ca^{2+} deregulation always precedes and determines somatic deregulation in neuronal cultures has not yet been directly established.

The above is not to deny the critical importance of Ca^{2+} overload to ultimate neuronal injury. Limiting Ca^{2+} influx during glutamate exposure has been shown by numerous studies to be neuroprotective against cell death (Choi, 1988b; Arundine and Tymianski, 2003), and, indeed, this study clearly shows that Ca^{2+} elevations were required ultimately for cellular injury (Fig. 4*B*). Once established, persistently high Ca^{2+} increases may trigger numerous Ca^{2+}-dependent processes that are critical for the full expression of neuronal injury. However, the present work suggests that triggering these processes can be dependent on dendritic mechanisms upstream of Ca^{2+} overload.

References

Arundine M, Tymianski M (2003) Molecular mechanisms of calcium-dependent neurodegeneration in excitotoxicity. Cell Calcium 34:325–337.

Attwell D, Laughlin SB (2001) An energy budget for signaling in the grey matter of the brain. J Cereb Blood Flow Metab 21:1133–1145.

Avignone E, Frenguelli BG, Irving AJ (2005) Differential responses to NMDA receptor activation in rat hippocampal interneurons and pyramidal cells may underlie enhanced pyramidal cell vulnerability. Eur J Neurosci 22:3077–3090.

Bindokas VP, Miller RJ (1995) Excitotoxic degeneration is initiated at non-random sites in cultured rat cerebellar neurons. J Neurosci 15:6999–7011.

Brocard JB, Tassetto M, Reynolds IJ (2001) Quantitative evaluation of mitochondrial calcium content in rat cortical neurones following a glutamate stimulus. J Physiol (Lond) 531:793–805.

Budd SL, Nicholls DG (1996) Mitochondria, calcium regulation, and acute glutamate excitotoxicity in cultured cerebellar granule cells. J Neurochem 67:2282–2291.

Castilho RF, Hansson O, Ward MW, Budd SL, Nicholls DG (1998) Mitochondrial control of acute glutamate excitotoxicity in cultured cerebellar granule cells. J Neurosci 18:10277–10286.

Chen QX, Perkins KL, Choi DW, Wong RK (1997) Secondary activation of a cation conductance is responsible for NMDA toxicity in acutely isolated hippocampal neurons. J Neurosci 17:4032–4036.

Chinopoulos C, Tretter L, Rozsa A, Adam-Vizi V (2000) Exacerbated responses to oxidative stress by an Na^+ load in isolated nerve terminals: the role of ATP depletion and rise of $[Ca^{2+}]_i$. J Neurosci 20:2094–2103.

Chinopoulos C, Connor JA, Shuttleworth CW (2007) Emergence of a spermine-sensitive, non-inactivating conductance in mature hippocampal CA1 pyramidal neurons upon reduction of extracellular Ca^{2+}: dependence on intracellular Mg^{2+} and ATP. Neurochem Int 50:148–158.

Choi DW (1988a) Glutamate neurotoxicity and diseases of the nervous system. Neuron 1:623–634.

Choi DW (1988b) Calcium-mediated neurotoxicity: relationship to specific channel types and role in ischemic damage. Trends Neurosci 11:465–469.

Connor JA, Cormier RJ (2000) Cumulative effects of glutamate microstimulation on Ca^{2+} responses of CA1 hippocampal pyramidal neurons in slice. J Neurophysiol 83:90–98.

Connor JA, Wadman WJ, Hockberger PE, Wong RK (1988) Sustained dendritic gradients of Ca^{2+} induced by excitatory amino acids in CA1 hippocampal neurons. Science 240:649–653.

Deshpande LS, Limbrick DD, Sombati S, Delorenzo RJ (2007) Activation of a novel injury-induced calcium permeable channel that plays a key role in causing extended neuronal depolarization and initiating neuronal death in excitotoxic neuronal injury. J Pharmacol Exp Ther 322:443–452.

Dietz RM, Kiedrowski L, Shuttleworth CW (2007) Contribution of Na^+/Ca^{2+} exchange to excessive Ca^{2+} loading in dendrites and somata of CA1 neurons in acute slice. Hippocampus 17:1049–1059.

Fischer G, Mutel V, Trube G, Malherbe P, Kew JN, Mohacsi E, Heitz MP, Kemp JA (1997) Ro 25–6981, a highly potent and selective blocker of *N*-methyl-D-aspartate receptors containing the NR2B subunit. Characterization in vitro. J Pharmacol Exp Ther 283:1285–1292.

Fried E, Amorim P, Chambers G, Cottrell JE, Kass IS (1995) The importance of sodium for anoxic transmission damage in rat hippocampal slices: mechanisms of protection by lidocaine. J Physiol (Lond) 489:557–565.

Greenwood SM, Mizielinska SM, Frenguelli BG, Harvey J, Connolly CN (2007) Mitochondrial dysfunction and dendritic beading during neuronal toxicity. J Biol Chem 282:26235–26244.

Grynkiewicz G, Poenie M, Tsien RY (1985) A new generation of Ca^{2+} indicators with greatly improved fluorescence properties. J Biol Chem 260:3440–3450.

Hori N, Carpenter DO (1994) Transient ischemia causes a reduction of Mg^{2+} blockade of NMDA receptors. Neurosci Lett 173:75–78.

Hoyt KR, Arden SR, Aizenman E, Reynolds IJ (1998a) Reverse Na^+/Ca^{2+} exchange contributes to glutamate-induced intracellular Ca^{2+} concentration increases in cultured rat forebrain neurons. Mol Pharmacol 53:742–749.

Hoyt KR, Stout AK, Cardman JM, Reynolds IJ (1998b) The role of intracellular Na^+ and mitochondria in buffering of kainate-induced intracellular free Ca^{2+} changes in rat forebrain neurones. J Physiol (Lond) 509:103–116.

Jekabsons MB, Nicholls DG (2004) In situ respiration and bioenergetic status of mitochondria in primary cerebellar granule neuronal cultures exposed continuously to glutamate. J Biol Chem 279:32989–33000.

Johnson-Cadwell LI, Jekabsons MB, Wang A, Polster BM, Nicholls DG (2007) "Mild Uncoupling" does not decrease mitochondrial superoxide levels in cultured cerebellar granule neurons but decreases spare respiratory capacity and increases toxicity to glutamate and oxidative stress. J Neurochem 101:1619–1631.

Kang Y, Notomi T, Saito M, Zhang W, Shigemoto R (2004) Bidirectional

interactions between h-channels and Na^+-K^+ pumps in mesencephalic trigeminal neurons. J Neurosci 24:3694–3702.

Kiedrowski L (2007) Critical role of sodium in cytosolic [Ca^{2+}] elevations in cultured hippocampal CA1 neurons during anoxic depolarization. J Neurochem 100:915–923.

Kiedrowski L, Wroblewski JT, Costa E (1994) Intracellular sodium concentration in cultured cerebellar granule cells challenged with glutamate. Mol Pharmacol 45:1050–1054.

Liu Y, Wong TP, Aarts M, Rooyakkers A, Liu L, Lai TW, Wu DC, Lu J, Tymianski M, Craig AM, Wang YT (2007) NMDA receptor subunits have differential roles in mediating excitotoxic neuronal death both *in vitro* and *in vivo*. J Neurosci 27:2846–2857.

Nicholls DG, Johnson-Cadwell L, Vesce S, Jekabsons M, Yadava N (2007) Bioenergetics of mitochondria in cultured neurons and their role in glutamate excitotoxicity. J Neurosci Res 85:3206–3212.

Novelli A, Reilly JA, Lysko PG, Henneberry RC (1988) Glutamate becomes neurotoxic via the *N*-methyl-D-aspartate receptor when intracellular energy levels are reduced. Brain Res 451:205–212.

Olney JW (1978) Neurotoxicity of excitatory amino acids. In: Kainic acid as a tool in neurobiology (McGreer EG, Olney JW, McGreer PL, eds), pp 95–121. New York: Raven.

Olney JW, Price MT, Samson L, Labruyere J (1986) The role of specific ions in glutamate neurotoxicity. Neurosci Lett 65:65–71.

Patton C, Thompson S, Epel D (2004) Some precautions in using chelators to buffer metals in biological solutions. Cell Calcium 35:427–431.

Petrozzino JJ, Connor JA (1994) Dendritic Ca^{2+} accumulations and metabotropic glutamate receptor activation associated with an *N*-methyl-D-aspartate receptor-independent long-term potentiation in hippocampal CA1 neurons. Hippocampus 4:546–558.

Pinelis VG, Segal M, Greenberger V, Khodorov BI (1994) Changes in cytosolic sodium caused by a toxic glutamate treatment of cultured hippocampal neurons. Biochem Mol Biol Int 32:475–482.

Randall RD, Thayer SA (1992) Glutamate-induced calcium transient triggers delayed calcium overload and neurotoxicity in rat hippocampal neurons. J Neurosci 12:1882–1895.

Rego AC, Ward MW, Nicholls DG (2001) Mitochondria control AMPA/kainate receptor-induced cytoplasmic calcium deregulation in rat cerebellar granule cells. J Neurosci 21:1893–1901.

Reyes M, Reyes A, Opitz T, Kapin MA, Stanton PK (1998) Eliprodil, a non-competitive, NR2B-selective NMDA antagonist, protects pyramidal neurons in hippocampal slices from hypoxic/ischemic damage. Brain Res 782:212–218.

Rothman SM (1985) The neurotoxicity of excitatory amino acids is produced by passive chloride influx. J Neurosci 5:1483–1489.

Scanlon JM, Brocard JB, Stout AK, Reynolds IJ (2000) Pharmacological investigation of mitochondrial Ca^{2+} transport in central neurons: studies with CGP-37157, an inhibitor of the mitochondrial Na^+-Ca^{2+} exchanger. Cell Calcium 28:317–327.

Shuttleworth CW, Connor JA (2001) Strain-dependent differences in calcium signaling predict excitotoxicity in murine hippocampal neurons. J Neurosci 21:4225–4236.

Simon RP, Swan JH, Griffiths T, Meldrum BS (1984) Blockade of *N*-methyl-D-aspartate receptors may protect against ischemic damage in the brain. Science 226:850–852.

Stout AK, Raphael HM, Kanterewicz BI, Klann E, Reynolds IJ (1998) Glutamate-induced neuron death requires mitochondrial calcium uptake. Nat Neurosci 1:366–373.

Vesce S, Jekabsons MB, Johnson-Cadwell LI, Nicholls DG (2005) Acute glutathione depletion restricts mitochondrial ATP export in cerebellar granule neurons. J Biol Chem 280:38720–38728.

Wadman WJ, Connor JA (1992) Persisting modification of dendritic calcium influx by excitatory amino acid stimulation in isolated Ca1 neurons. Neuroscience 48:293–305.

Wahlestedt C, Golanov E, Yamamoto S, Yee F, Ericson H, Yoo H, Inturrisi CE, Reis DJ (1993) Antisense oligodeoxynucleotides to NMDA-R1 receptor channel protect cortical neurons from excitotoxicity and reduce focal ischaemic infarctions. Nature 363:260–263.

Wilding TJ, Huettner JE (1995) Differential antagonism of alpha-amino-3-hydroxy-5-methyl-4- isoxazolepropionic acid-preferring and kainate-preferring receptors by 2,3-benzodiazepines. Mol Pharmacol 47:582–587.

Williams K (1993) Ifenprodil discriminates subtypes of the *N*-methyl-D-aspartate receptor: selectivity and mechanisms at recombinant heteromeric receptors. Mol Pharmacol 44:851–859.

Yamaguchi K, Ohmori H (1990) Voltage-gated and chemically gated ionic channels in the cultured cochlear ganglion neurone of the chick. J Physiol (Lond) 420:185–206.

Zhang Y, Lipton P (1999) Cytosolic Ca^{2+} changes during *in vitro* ischemia in rat hippocampal slices: major roles for glutamate and Na^+-dependent Ca^{2+} release from mitochondria. J Neurosci 19:3307–3315.

Zhou M, Baudry M (2006) Developmental changes in NMDA neurotoxicity reflect developmental changes in subunit composition of NMDA receptors. J Neurosci 26:2956–2963.